

Ultrathin metal films on a metal oxide surface: Growth of Au on TiO₂ (110)

Lei Zhang, Rajendra Persaud,* and Theodore E. Madey†

Department of Physics and Astronomy, and Laboratory for Surface Modification, Rutgers, The State University of New Jersey, Piscataway, New Jersey 08855

(Received 12 June 1997)

We have studied the growth of ultrathin Au films on the TiO₂ (110) surface using low-energy ion scattering (LEIS), x-ray photoelectron spectroscopy (XPS), and low-energy electron diffraction (LEED). For substrate temperatures of 160 and 300 K, for fractional monolayer Au coverages, Au evaporated under UHV conditions appears to grow initially on the stoichiometric TiO₂ (110) surface in a quasi-two-dimensional (2D) form. As the average Au coverage increases to one monolayer (1 ML) and higher, Au forms three-dimensional (3D) islands. The coverage at which 3D islands become apparent in LEIS data decreases as the surface temperature increases. No evidence of significant chemical interactions has been found between the Au and TiO₂ substrate. By annealing Au/TiO₂ to temperatures up to 775 K, the Au islands continue to grow; encapsulation of the Au islands by Ti suboxides is not observed. There is little or no CO adsorption on small Au clusters at 300 K (upper limit of ~0.05 ML), based on sensitive LEIS measurements. [S0163-1829(97)08740-7]

I. INTRODUCTION

In recent years, metal-on-oxide systems have received considerable attention because of their importance in a variety of applications. These include the fabrication of new ceramic materials, heterogeneous catalysts,¹ and solid-state gas sensors.² A detailed understanding of the processes occurring at the metal/oxide interfaces and their correlation to the properties of materials and devices could lead to improvements in efficiency and performance.

We have chosen TiO₂ as the oxide substrate for this study for several reasons. First, the electronic structure of TiO₂ has been well characterized and surface stoichiometry can be established under UHV conditions. Moreover, TiO₂ has been used in semiconductor gas sensor devices,^{2,3} but the sensing mechanism is unclear and many challenging scientific problems still remain. We thus have a twofold purpose to our study; first, from a basic point of view, to understand noble metal/oxide surfaces and their interfacial reactivity, and second, from an applied point of view, to understand the correlation of material properties to practical applications, such as gas sensors.

The present study is part of a systematic investigation of the growth of different metals (including Cr, Fe, Cu, Hf, and Pt) on TiO₂ (110);⁴⁻⁹ for a recent review of metals on TiO₂, see Ref. 10. The Au/TiO₂ system is investigated because it has the potential to be a good chemical gas sensor and can act as a catalyst for the room-temperature oxidation of CO.¹¹⁻¹³ The catalytic activity for CO oxidation as well as the gas sensing properties seem to depend on both the small grain size of Au and the choice of support oxides.^{11,14} In addition, there is some speculation that the reactivity of Au towards oxygen may depend on the dimensions of Au clusters.¹⁵ Since the surface of pure gold is known to be unreactive to most gases, including CO and O₂, much basic information is needed to interpret these unusual and interesting results.

We present here a detailed description of the interaction of Au with TiO₂ (110). Comparing our results with the

Pt/TiO₂ (110) system,⁸ it has been found that, during later stage growth (average overlayer thicknesses >1 ML), at equivalent coverages (Au and Pt) and temperatures, more of the TiO₂ (110) surface is covered by Pt islands than by Au, i.e., Pt wets TiO₂ (110) better than Au. In addition, annealing of Au/TiO₂ to temperatures up to 775 K results in an increase in the size of the Au islands, with no significant encapsulation. This is in contrast to the Pt/TiO₂ (110) system, for which complete encapsulation by TiO_x (0 < x < 2) is observed under equivalent conditions.^{8,16,17} Moreover, we find little or no evidence for CO adsorption on Au clusters at 300 K [upper limit of ~0.05 ML for 600 L (1 L = 10⁻⁶ Torr s CO exposure)], based on sensitive low-energy ion scattering (LEIS) measurements.

II. EXPERIMENT

The experiments are performed in an ultrahigh vacuum (UHV) system, as described in detail elsewhere.¹⁸ The base pressure of the chamber is less than ~2 × 10⁻¹⁰ Torr. The chamber contains a VSW x-ray source that can generate either Al Kα or Mg Kα radiation for x-ray photoelectron spectroscopy (XPS), a quadrupole mass spectrometer (QMS) used for residual gas analysis, an electron gun (0–1000 eV) and a sensitive two-dimensional retarding field detector (two grids, microchannel plate assembly and phosphor screen) used for low- and medium-energy electron diffraction (LEED and MEED). The chamber is additionally equipped with a differentially pumped ion gun used for low-energy ion scattering and Ar⁺ sputtering, and a 100-mm radius hemispherical analyzer used in the fixed analyzer transmission mode for XPS and the fixed retardation ratio mode for LEIS.

The freshly polished sample is a 5 × 10 × 1 mm³ TiO₂ single crystal with (110) orientation obtained from Commercial Crystal Laboratories. The sample is attached to a Ta foil holder, and mounted on a XYZ rotary manipulator. The sample is heated through a combination of radiation and electron bombardment using a tungsten filament positioned

behind it. A W 5%Re/W 26% Re thermocouple spot welded on the Ta foil very close to the sample is used for temperature measurements. The sample is partially reduced by annealing at ~ 1000 K in a UHV chamber for ~ 1 h. After this treatment, the bulk becomes an *n*-type semiconductor; this eliminates any charging problems in XPS and LEIS measurements. The sample, initially transparent, becomes dark blue after extensive reduction. The TiO_2 surface stoichiometry, determined using XPS, is restored by bombarding for ~ 30 min with 1-keV Ar^+ ions (ion beam rastered across the sample, current density $\sim 1 \times 10^{-5}$ A/cm²), followed by a 10-min anneal at 975 K in 10^{-6} Torr oxygen. After annealing, the sample is allowed to cool for 10 min in the same oxygen ambient pressure. Full details of the sample treatment are described elsewhere.¹⁹ The clean stoichiometric surface produces a sharp LEED (1×1) pattern.

The Au films are deposited by thermal evaporation from a shielded liquid-nitrogen-cooled metal source. The deposition rate is 0.5–0.8 Å/min. During evaporation, the pressure in the chamber increases to about 3×10^{-10} Torr. The average thickness of the metal films is determined using a quartz crystal monitor (QCM), which has been calibrated using Rutherford backscattering spectroscopy (RBS). All thicknesses reported in this paper are average thicknesses. Here 1 ML refers to the amount of Au [arranged in the close-packed (111) structure] required to cover the substrate with a single atomic layer; for Au with bulk density of 19.3 g/cm³, the thickness of such a layer is ~ 2.6 Å.

XPS spectra are obtained using both normal (0°) and grazing angle emission (70° with respect to the surface normal). Compared with normal emission XPS, grazing angle XPS is much more surface sensitive. Since the attenuation length of photoelectrons is very short (10–20 Å), the electron escape depth is limited to the top few atomic layers of the solid for grazing angle XPS. For normal angle XPS, a larger fraction of the photoelectrons originate deeper in the bulk of the sample.

The low-energy ion scattering technique, in which He^+ ions having kinetic energies ~ 1 keV are scattered from a surface, is extremely sensitive to the composition of the top-most layer of the surface.^{20,21} In our experiments, the probe ions are 1.0-keV He^+ and the scattering angle is fixed at 135° . A typical LEIS spectrum is obtained in ~ 4 min at an average He^+ bombardment current of $\sim 2 \times 10^{-7}$ A/cm² (total dose of $\sim 3 \times 10^{14}$ ions/cm²). The total ion beam exposure is low enough that beam damage is minimal.¹⁹

III. RESULTS

A. Thin-film growth mode

Under conditions of thermodynamic equilibrium, the growth mode for film *F* on substrate *S* can be classified according to their surface and interfacial energies (γ_F , γ_S , and γ_{FS} , respectively).¹⁰ If $\Delta\gamma = \gamma_F + \gamma_{FS} - \gamma_S \leq 0$, then growth will proceed in a layer-by-layer behavior (Frank–van der Merwe mode, FM); if $\Delta\gamma > 0$, then the film will grow three dimensionally (Volmer–Weber growth, VW). In many cases, an increase in the interfacial energy ($\Delta\gamma \leq 0 \rightarrow \Delta\gamma > 0$) after the completion of a layer or layers can lead to the subsequent formation of islands. This third mode is referred to as the Stranski–Krastanov growth mode [SK, layer(s) fol-

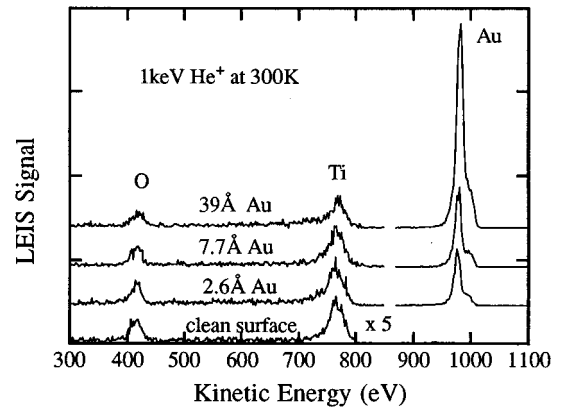


FIG. 1. LEIS spectra for Au/TiO_2 (110) deposited at room temperature for different average Au coverages.

lowed by islands]. In many practical situations, including ours, the growth studies are performed under conditions far from equilibrium where kinetics rather than thermodynamics determine the final film morphology;²² however, this classification continues to be an effective guideline in growth studies.

LEIS can be used to distinguish between an initial three-dimensional and an initial layerlike form of growth (FM or SK).⁷ If the growth mode is FM or SK, the intensity of He^+ scattered from overlayer atoms increases linearly with overlayer coverage, reaching a plateau at the completion of the first monolayer (1 ML). The substrate intensity simultaneously decreases linearly and is completely attenuated above 1 ML. This effect has been observed in our previous studies of Fe/TiO_2 (Ref. 6) and Hf/TiO_2 (Ref. 5) for growth at 160 K and room temperature, respectively. In the case of the VW (cluster) growth mode, the relationship between He^+ scattering intensity and metal overlayer coverage is expected to be a smooth, nonlinear function. Since the substrate is still exposed after deposition of a few ML, the overlayer signal still increases and the substrate signal is nonzero. This behavior has been observed for Cu (Ref. 7) and Pt (Ref. 8) on TiO_2 . It should be emphasized that LEIS cannot distinguish between the FM and SK growth modes in which the surface is completely covered by the first ML.

LEIS spectra obtained using 1-keV He^+ after room-temperature deposition of Au on TiO_2 (110) are shown as a function of average Au thickness in Fig. 1. The bottom spectrum represents the clean TiO_2 substrate with the Ti peak appearing at 760 eV and O at 420 eV. Upon Au deposition, a peak due to Au appears at 980 eV. The intensity of this peak increases with average Au thickness while those of both Ti and O decrease.

Figures 2(a), 2(b), and 2(c) show the integrated He^+ intensities of Au, Ti, and O as a function of average Au thickness obtained after deposition onto TiO_2 (110) at 300 K. Each data point corresponds to the integrated intensity averaged over several experiments. The error bars represent the standard deviation about the mean. The error in reproducing the average thickness is too small to be displayed. The dashed lines in the figure indicate the intensity versus coverage behavior expected for two-dimensional growth. During

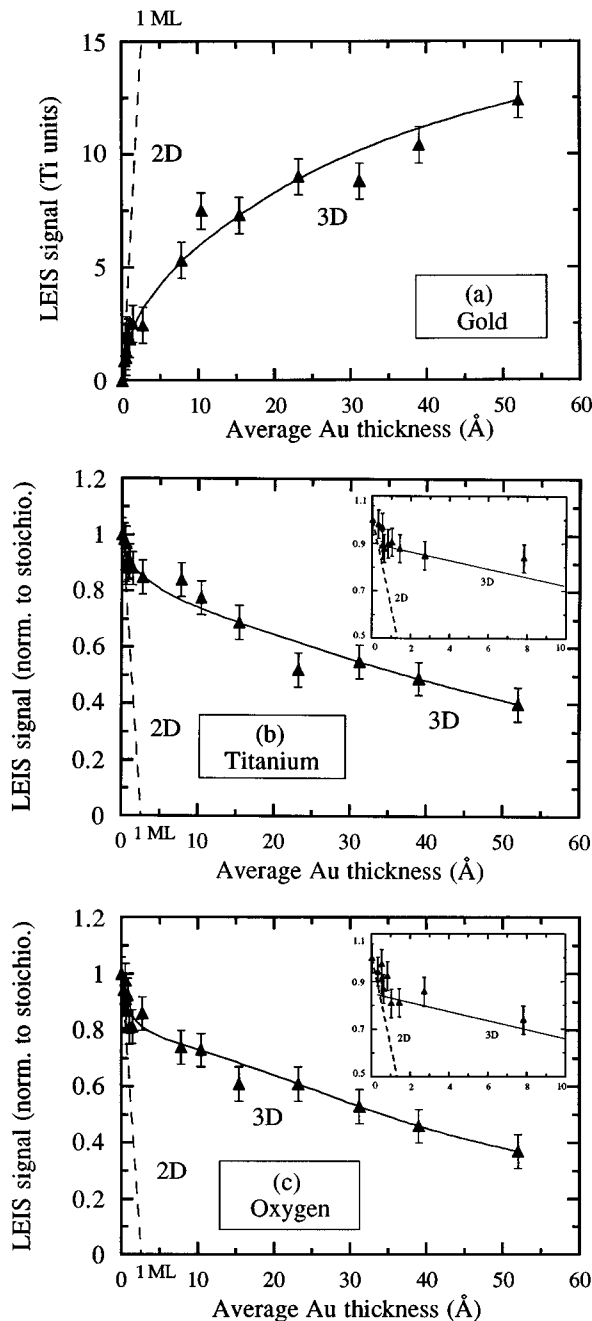


FIG. 2. LEIS intensities of (a) gold; (b) titanium; (c) oxygen vs the average Au thickness. Au, O, and Ti intensities are normalized to the Ti intensity of the stoichiometric surface. The solid lines are guides for the eye. The dashed lines indicate the expected two-dimensional growth behavior. The insets show low coverage data on expanded scales.

initial stage growth for fractional monolayer Au coverage, the substrate Ti and O signals change along a slope very close to that expected for two-dimensional (2D) growth (dashed lines), within $\sim \pm 5\%$ deviation [note the low-coverage data are plotted on expanded scales as insets to Figs. 2(b) and 2(c)]. Simultaneously, the Au signal increases with a slope also close to that expected for 2D growth (dashed lines); there exists a break point at fractional monolayer Au coverage. These data indicate that Au grows initially as 2D islands, or as flat 3D islands at fractional mono-

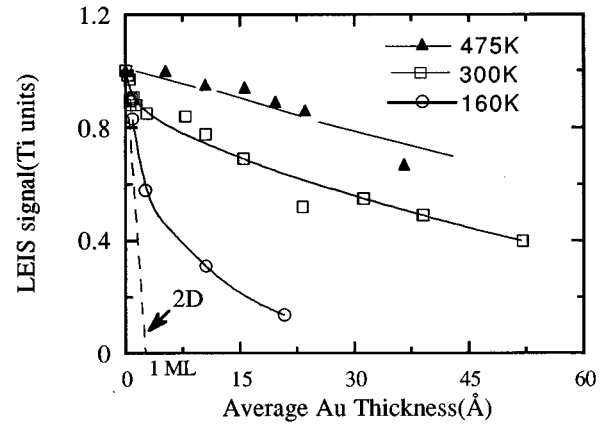


FIG. 3. Deposition of Au at 160, 300, and 475 K. LEIS Ti intensity vs average Au thickness. Lines are guides for the eye.

layer coverage; we call this quasi-2D growth. As the average Au thickness increases to 1 ML and above, both the substrate and overlayer signals deviate from the 2D dashed lines, exhibiting behavior indicative of 3D island formation. At the break point where the transition from quasi-2D to 3D occurs, the substrate Ti and O signals drop by about 15%; this implies that the apparent coverage for the quasi-2D \rightarrow 3D transition is about 0.15 ML. Even at about 40 Å average Au coverage, the Ti intensity is reduced only by $\sim 50\%$. This means that 50% of the substrate remains uncovered, and is a clear indication that Au grows in the form of three-dimensional clusters on the TiO_2 substrate at room temperature.

B. Growth of Au/ TiO_2 at different substrate temperature

To investigate the effect of temperature on the growth mode of the clusters, we have also performed LEIS experiments for Au deposition at 160 and 475 K. Plots of the integrated Ti intensities as a function of average Au thickness for substrate temperatures of 160, 300, and 475 K are superimposed in Fig. 3. The results show that for substrate temperatures of 160 and 300 K and for fractional monolayer Au coverage, the Ti signals decrease initially at the rate close to that expected for 2D growth behavior. As indicated above, this implies that Au grows in a quasi-2D fashion at very low coverages both at 160 and 300 K. After 1 ML, even at 160 K, the growth is three dimensional; however, a larger fraction of substrate area is covered by Au at 160 K than 300 K for equivalent Au coverage. At 475 K, the growth appears to be 3D from the beginning. The general trend is that for higher substrate temperatures, less substrate area is covered. A similar phenomenon has been observed for the Pt/ TiO_2 (110) system.⁸

C. XPS investigation of interfacial reaction

X-ray photoelectron spectroscopy can be used to investigate the interfacial interactions between thin films and substrate, including metal-oxide interactions and metal-metal interactions. In XPS, an oxidized metal state generally gives core-level photoemission at a higher binding energy than the corresponding metallic state.²³

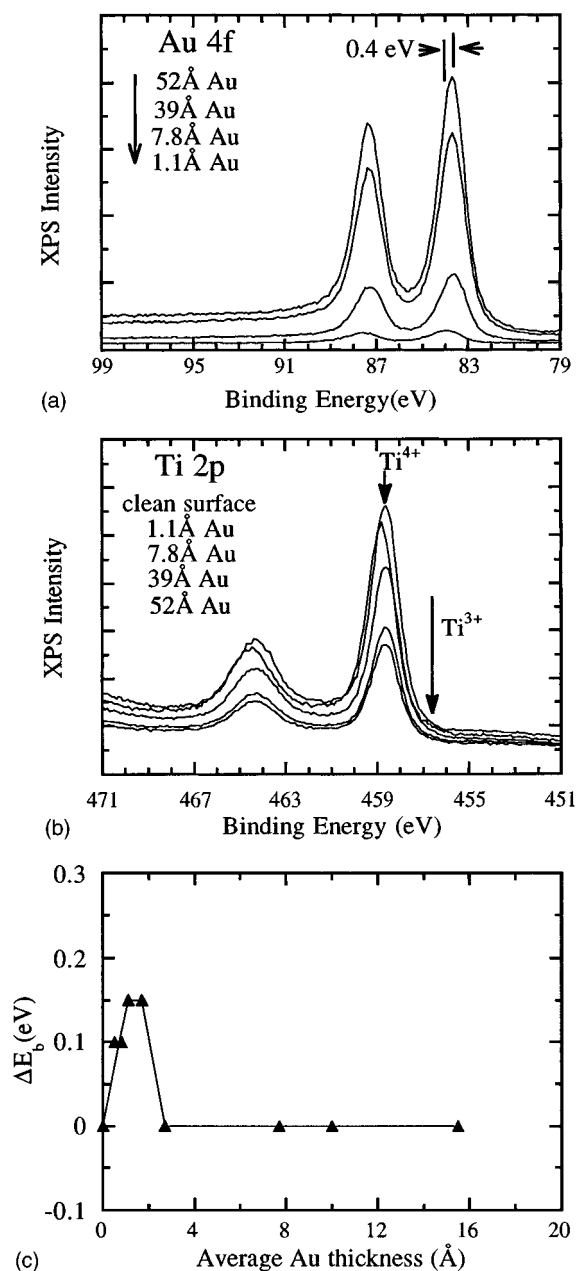


FIG. 4. XPS spectra of (a) Au 4*f*; (b) Ti 2*p* for different Au thicknesses between 1.1 and 52 Å. Au was deposited at room temperature. (c) Binding energy shifts of the Ti 2*p* core level peak are plotted as a function of average Au thickness.

Figures 4(a) and 4(b) show the XPS spectra of Au 4*f* and Ti 2*p*, respectively. During the initial growth, the Au 4*f* peak is shifted to the high-binding-energy side by 0.4 eV. In principle, such a shift for an overlayer metal may be related either to the oxidation of the overlayer metal or to an electron screening effect due to variations in Au cluster size with average film thickness. Since oxidation of the overlayer metal could be accompanied by reduction of the substrate cations, reduced Ti oxide peaks should appear if the overlayer were oxidized. The binding energies of the Ti³⁺ and Ti²⁺ peaks are 1.8 and 3.6 eV lower than that of the Ti⁴⁺ peak, respectively.⁹ As displayed in Fig. 4(b), no indication of photoemission from a reduced Ti^{δ+} ($0 \leq \delta < +4$) species has been found in the Ti 2*p* XPS spectra. Based on these

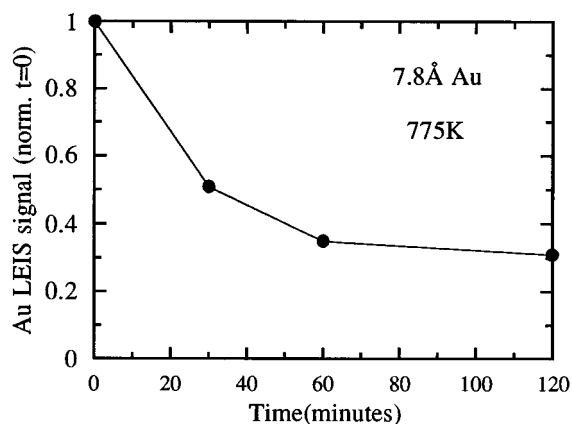


FIG. 5. Evolution of the Au LEIS intensity as a function of accumulated annealing time, for 7.8-Å-thick Au layers at 775 K. Intensities are normalized to the “as-deposited” value.

observations, we rule out an oxidation effect, and instead relate the shift of the Au 4*f* peak at low Au coverages to reduced coordination in small Au clusters and electron screening effects. A similar conclusion was reached for Cu/TiO₂.⁷ Note that Au is not expected to be oxidized: there is no evidence in the literature for dissociative adsorption of O₂ on a clean Au surface,²⁴ although metallic Au can be oxidized to Au₂O₃ by exposure to ozone and UV irradiation.²⁵

For very low Au coverages (~ 1 Å), the Ti 2*p* peak is shifted to the high-binding-energy side by a very small amount (about 0.1–0.2 eV); note the 1.1-Å curve in Fig. 4(b). This shift is reproducible for low average Au coverage and the change of the binding energy is plotted as a function of average Au thicknesses in Fig. 4(c). A similar shift has been observed for the O 1*s* peak. These observations appear to be due to band bending,²⁶ as discussed in Sec. IV A.

Besides the small peak shifts for Ti 2*p* and Au 4*f* at the initial stage of growth, there are no further changes in peak shape or position, so there is no evidence of strong interaction between Au and the substrate.

D. Annealing effects

For Cu on TiO₂ (110),⁷ it has been shown that annealing in UHV can cause a change in morphology of Cu particles so as to expose more TiO₂ surface. For other metals on TiO₂ (110), such as Pt and Fe, it has been found that annealing in UHV leads to encapsulation, where reduced Ti oxides migrate to cover the metal clusters.^{27,28} This is commonly associated with the “strong metal-support interaction (SMSI)” effect in catalysis.²⁹ In order to determine the thermal stability of Au/TiO₂ and search for evidence of encapsulation, we have carried out the following experiments.

Following deposition of a 7.8-Å Au film, XPS and LEIS measurements are made. Then, the sample is heated for a given time, after which XPS and LEIS measurements are carried out at room temperature; a series of successive annealing and measurement steps are followed.²⁸ The LEIS measurements for 7.8-Å Au/TiO₂ annealed at 775 K are displayed as a function of accumulated annealing time in Fig. 5. The Au signal decreases as a function of annealing time;

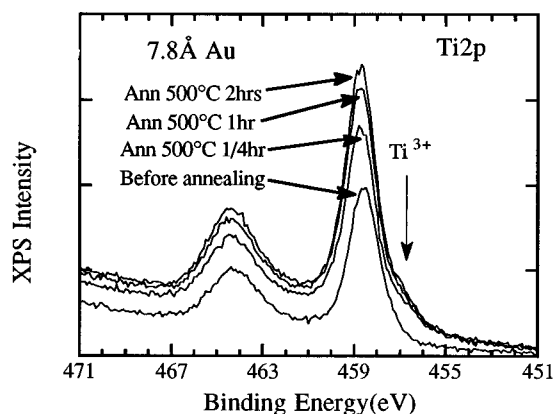


FIG. 6. XPS spectra of Ti 2*p* for 7.8-Å Au layer, annealed at 775 K.

after 1 h, the Au signal reaches a steady-state value, which is 30% of the original Au intensity before annealing, while both Ti and O signals have increased as a function of annealing time.

Grazing angle XPS experimental results obtained before each LEIS measurement described above are displayed in Fig. 6. The feature appearing at the low-binding-energy side of the XPS Ti 2*p* peak is due to the presence of reduced Ti species.

There are different explanations consistent with the data of Figs. 5 and 6. The clusters could be encapsulated by TiO_x ($0 < x < 2$) suboxides, or they could simply grow thicker or larger and expose more TiO_2 . The appearance of reduced TiO_x seems to support encapsulation, but we are able to rule out this interpretation by the following experiments. We annealed the clean, stoichiometric TiO_2 substrate at 775 K for 15 min. The grazing angle XPS Ti 2*p* spectra are displayed in Fig. 7. By decomposing the Ti 2*p* peaks into fully oxidized Ti and reduced Ti components using a curve fitting procedure, we have found that the contribution of the reduced Ti saturates at about the same Ti 2*p* intensity for annealed stoichiometric TiO_2 as for annealed Au/ TiO_2 systems.

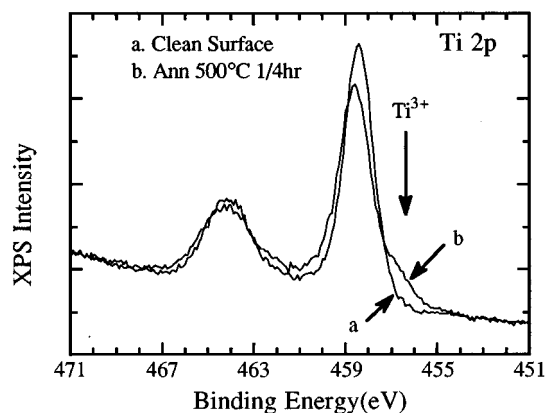


FIG. 7. XPS spectra of Ti 2*p* of stoichiometric TiO_2 surface (solid line) and annealed surface at 775 K (dashed line).

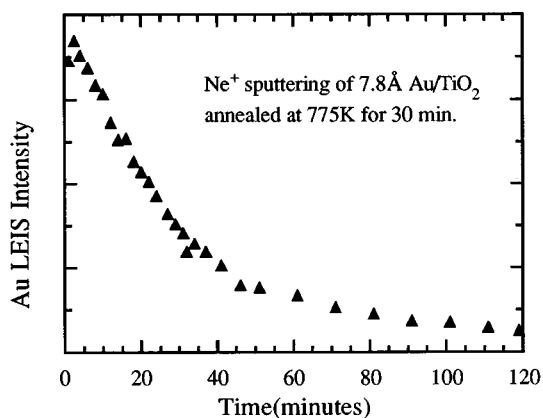


FIG. 8. The Au LEIS intensity as a function of the Ne^+ sputtering time. Average Au thickness is 7.8 Å; surface is annealed to 775 K for 1/2 hour prior to this measurement.

If the Au clusters were encapsulated with suboxides, then the LEIS signal from Au should increase after the suboxides have been sputtered off. Neon is an ideal choice as the probe ion in these experiments as it can sputter the overlayer effectively due to its large mass (as compared to He) while retaining a sensitivity to Au in LEIS. The experimental result obtained from Ne^+ sputtering and LEIS of 7.8-Å Au/ TiO_2 , which had previously been annealed at 775 K for 30 min is shown in Fig. 8. When the sample is exposed to a continuous dose of Ne^+ ions, the Au signal slowly decreases. This corresponds to the removal of Au overlayers by Ne^+ sputtering.

Combining the above XPS results with the Ne^+ sputtering and LEIS results, one can conclude that there is no significant encapsulation of the Au islands. Instead, due to either island growth (e.g., Ostward ripening) or island thickening, less substrate area is covered by Au after annealing. Recent high-resolution scanning electron microscopy (HRSEM) studies of 50-Å Au/ TiO_2 annealed at 475 K support an island thickening model.³⁰ Mass conservation implies that island thickening is accompanied by a decrease in the substrate area covered by Au islands; island thickening is consistent with a decrease in the LEIS Au intensity and a simultaneous increase of Ti and O intensities upon annealing (Fig. 5). The formation of the reduced Ti suboxide is mainly a consequence of annealing TiO_2 to $T > 775$ K.

E. The adsorption of CO on Au/ TiO_2

As indicated in the Introduction, Au clusters on selected support oxides (such as TiO_2 , Fe_2O_3) have shown a high catalytic activity for carbon monoxide (CO) oxidation.^{12,14} CO and O_2 are not observed to adsorb on planar Au surfaces at room temperature,²⁴ and it has been speculated that small Au clusters have enhanced reactivity towards CO.^{11,14} In order to search for evidence of reactivity between small Au clusters and CO, we have performed an investigation of chemisorption of CO on Au/ TiO_2 at room temperature for different Au coverages, using low-energy ion scattering.

The idea behind this experiment is as follows: LEIS has high sensitivity for detection of Au on TiO_2 (Fig. 1). If CO adsorbs on Au, the Au LEIS signal will decrease due to "blocking" of the substrate Au by the adsorbed molecules,

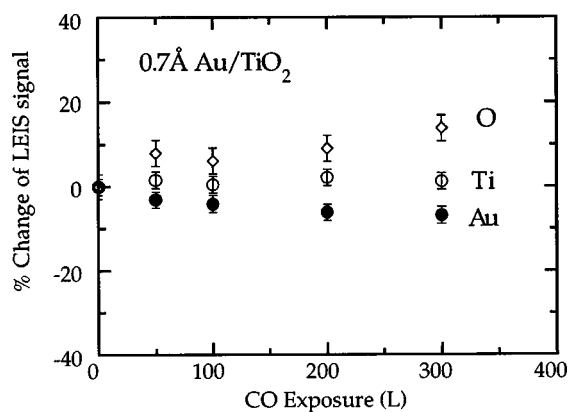


FIG. 9. The percentage change of LEIS intensities of Au, Ti, and O as a function of CO exposure for 0.7-Å AuTiO₂ system at 300 K.

so that the probability of He⁺ scattering from Au is reduced.¹⁹ Even for very low CO coverages (<0.1 ML) on a low density of small Au particles (<1 Å average thickness, giving <15% coverage of the TiO₂ surface by Au), one expects to find attenuation of the LEIS Au signal. It is difficult to detect CO on Au directly because of the high O background from TiO₂, and the small cross section for scattering from C, but this indirect detection by attenuation of Au should be very sensitive.

The experimental sequence that we have used to search for CO adsorption is as follows: the small Au particles, formed after deposition at 300-K substrate temperature, are then exposed to 1.0×10^{-6} Torr CO for different time periods (increasing CO exposure). The XPS as well as LEIS measurements are then performed to search for evidence of CO adsorption, with the substrate kept at room temperature.

The percentage changes of LEIS signal for Au, Ti, and O obtained from 0.7-Å Au/TiO₂ as a function of CO exposure are displayed in Fig. 9. The tiny gold clusters cover a small fraction of the TiO₂ surface at 0.7-Å average coverage thickness, at 300 K [cf. Fig. 2(b)]. Under a wide range of CO exposure, the Ti intensity remains almost unchanged; however, the Au intensity decreases and O intensity increases after exposure to CO. Similar results have been observed for the 1.0-Å Au/TiO₂ system. As indicated above, we suggest that the attenuation of the Au LEIS signal is due to the blocking of Au by adsorbed species. We conclude that there is little, if any, CO adsorption under these conditions. An upper limit on the CO coverage after a 300-L dose of CO is ~0.05 ML, and we cannot rule out the possible influence of adsorbed intensities. The increase in the O signal may indicate adsorption of an O-containing species on TiO₂, as well as Au.

A search for adsorption of oxygen on small Au clusters has been performed under the same conditions as above, for exposures of O₂ at substrate temperatures of 160 and 300 K. After exposures of 600-L O₂, at each temperature, both Au and Ti LEIS peak intensities decrease, while there is little or no change in the O LEIS signal. Considering the uncertainties in the measurements and possible impurity effects, we estimate the upper limit of O coverage on the Au to be similar to that of CO.

IV. DISCUSSION

A. The initial stage growth (<1 ML)

Based on LEIS measurements during the initial stage growth for fractional monolayer Au coverage, Au grows initially on a TiO₂ (110) substrate as 2D islands, or as flat 3D islands at 160 and 300 K. Ernst and co-workers²¹ have interpreted the evolution from 2D to 3D growth of metals on oxide surfaces in terms of the adatom adsorption and diffusion properties. Their model suggests that a strong attraction energy to the edge of the islands can cause deposited adatoms to stick to the edges of already formed nucleation centers. In the initial stages of film growth at 300 K and below, metal overlayers may grow as 2D islands until a critical island size is reached, at which point 3D growth begins. Ernst *et al.*²¹ report experimental evidence for a transition from 2D to 3D island growth for a fractional monolayer of Cu on ZnO. Our results for Au/TiO₂ (110) are qualitatively similar, in that a transition from quasi-2D growth to 3D is observed at fractional monolayer Au coverages [Figs. 2(b) and 2(c)]. Recent electron stimulated desorption (ESD) studies of O⁺ ions from Au/TiO₂ suggest that Au growth occurs initially at steps and defects as the quasi-2D layer forms.³¹ Evidence for 2D to 3D transitions in island growth has also been reported for Ag/TiO₂ (110) (Ref. 32) and Pt/TiO₂ (110).³³ It should be emphasized that the equilibrium growth mode for all of the above cases is expected to be the Volmer-Weber mode (3D clusters), based on the relative surface energies. The observation of 2D growth or quasi-2D growth at low coverages and low temperatures is a consequence of surface kinetic limitations.

When the Au coverages are less than 1 ML, the binding energy of the Ti 2*p* core-level peak is shifted to higher binding energy by 0.1 to 0.15 eV, and is shifted back to its original position after 1 ML, as shown in Fig. 4(c). Simultaneously, the O 1*s* peak shifts in the same manner under the above conditions. We interpret these effects as being due to band bending. On a clean semiconductor surface, extrinsic surface states can appear on the surface due to adsorption of foreign atoms (even a small concentration). In the present case, the adsorption of nanoscale Au clusters may cause the appearance of surface bound electronic states on TiO₂ (110). If the position of a surface state is above the Fermi level before thermodynamic equilibrium is reached, it will act as a donorlike state, and electrons will transfer from the surface state created by tiny Au clusters into the oxide substrate. This will cause the Au to become cationic and produce a negative space charge region in the TiO₂ after thermal equilibrium. The net result is that the energy bands are bent “downward” at the surface and the binding energy of the core level of Ti 2*p* is increased. This is consistent with the formation of an ideal Au-TiO₂ junction. Since the average work function of Au (4.83 eV) (Ref. 34) is lower than that of TiO₂ (5.3 eV),³⁵ electrons are expected to flow from Au metal to TiO₂ and result in downward band bending after contact. For average Au coverages of >1 ML, the Au clusters apparently are neutral and unpolarized, so that the Ti 2*p* and O 1*s* peaks appear at the values of the clean substrate. The observation of band bending at only the lowest Au coverages may be related to the initial nucleation of nanoscale Au clusters at the defect sites.

An appreciable band bending effect has been observed for fractional monolayer Cu deposited onto O-terminated ZnO (0001) substrate at 130 K.²¹ The Zn $2p_{2/3}$ peaks shift to higher binding energy; this is interpreted as being due to the donation of Cu electrons to the substrate. The evaporation of Cs on TiO₂ also causes downward band bending at fractional monolayer coverage.^{36,37} It is common for band bending to occur for fractional monolayers of metal on semiconductors, due to the creation of surface electronic states.

B. The later stages of growth (>1 ML)

Based on the LEIS data of Figs. 1–3, we conclude that Au grows on TiO₂ (110) in the Volmer-Weber mode in the range 160–475 K for high coverage; three-dimensional Au clusters are separated by areas of clean TiO₂. Based either on an island growth or island thickening model, the gold clusters grow larger and/or thicker with increasing temperature. At room temperature and 15 Å average Au coverage, the Ti intensity is reduced to $68 \pm 5\%$, indicating that only 32% of the substrate is covered by Au. At 52 Å, the Ti intensity decreases to $40 \pm 5\%$, implying that only about 60% of the TiO₂ substrate is covered by Au. So even at such a high average Au coverage, a large fraction of the substrate area is still exposed; this is clear evidence that the growth is three dimensional. Similar phenomena have been known for many years for Au on alkali halides;³⁸ Au forms clusters along the steps of the alkali halides to decorate the surface defects.

An independent estimate of the substrate area covered by Au has been obtained from HRSEM studies of the morphology of Au/TiO₂.³⁹ The Au depositions have been performed at 300 K under UHV conditions, then the samples have been transferred in air to the SEM chamber for imaging. Over a wide range of Au coverages from 2.2 to 50 Å, the HRSEM estimations are in excellent agreement with our LEIS results. This indicates that air exposure does not affect the surface area covered by Au. Based on these results, we can assume that the morphology of Au islands does not change due to the sample transfer in air. For low average Au thicknesses (<15 Å), Au forms 3D dropletlike islands. As the Au thicknesses increase (>15 Å), the Au islands become wormlike structures.³⁹

In order to determine whether or not the Au films are crystalline, LEED experiments have been performed on the 30- and 50-Å Au/TiO₂ systems, which are deposited at room temperature in UHV. Poorly developed hexagonal LEED patterns are obtained over a range of electron beam energies. This indicates that the Au overlayer has crystallized with a fcc structure and (111) orientation, although the epitaxial relationship between Au and TiO₂ are not nearly as well developed as for Cu/TiO₂,⁴ where sharp LEED patterns are observed. In addition to LEED, the electron backscattered diffraction (EBSD) technique has been applied in an HRSEM to determine both the orientation of the surface normal as well as the in-plane x and y direction of annealed Au clusters, with respect to the TiO₂ substrate.³⁹ Two domains corresponding to two epitaxial variants of Au clusters that are rotated by 180° have been determined, each with a distribution of normal directions along [111] that is parallel to

the [110] direction of TiO₂. The in-plane orientation of one of the domains corresponds to $[\bar{1}\bar{1}0]$ Au/[001] TiO₂, and the other to $[\bar{1}10]$ Au/[001] TiO₂.

A satisfactory model to explain the temperature-dependent LEIS data needs to describe the larger fraction of exposed TiO₂ surface for the same average Au coverage, as substrate temperature increases (Fig. 3). We consider two possibilities. One model to account for the above growth behavior is an island growth model,⁷ in which a smaller concentration of larger islands grows at high temperature. For growth at lower temperatures, kinetic effects dominate. Thermally activated diffusion of Au is reduced and a high density of small Au islands is nucleated. As the substrate temperature increases, some of the kinetic barriers are overcome and the clusters grow in size by a combination of Ostwald ripening (growth of larger clusters at the expense of smaller clusters⁴⁰) and coalescence (clusters merge). In this model, the density of islands decreases and the average island size increases with increasing temperature, so a smaller fraction of the substrate area would be covered by Au as the substrate temperature increases.

Another model that can also be used to interpret this phenomenon is an island thickening model developed by Campbell,³⁶ in which the concentration of the islands does not change much, but islands thicken and cover less area. As the second Au layer is formed on the top of the first layer of a cluster, it will reduce the up-step activation energy (Au migrates from TiO₂ sites to Au sites). As the substrate temperature increases, the up-step activation barrier is thermally accessible and upstepping can occur. The clusters become more narrow in size and thicker in height. So in the substrate temperature range between 160 and 475 K, Au islands could cover less substrate area for the same average Au thickness as the surface temperature increases. The relative contributions of the above two models, which give rise to the change of cluster shapes, are not possible to distinguish here in the absence of microscopic investigations. Our recent high-resolution scanning electron microscopy studies^{30,39} of 50 Å Au/TiO₂ deposited at 300-K substrate temperature show strong evidence of full coalescence at early stage growth and partial coalescence at later stage growth. Growth at higher substrate temperature (475 K) shows a bimodal cluster size distribution with large and small clusters; this may involve both thermally induced island thickening effects together with the Ostwald ripening and coalescence effects.

C. Comparison with Cu, Fe, and Pt/TiO₂ systems

In most growth studies of metals on oxide surfaces, the metal normally has higher surface free energy than the oxide. For example, the surface energy of Au (~1130 erg/cm²) (Ref. 25) is about 4 times larger than that of TiO₂ (280–380 erg/cm²). Metals are energetically favored to form clusters on oxide substrates at equilibrium if the interface free energy is small or positive. The fact that some metals “wet” TiO₂ [e.g., Fe,⁶ Cr,⁹ Hf (Ref. 5)] is related to a large, negative interface energy.

Based on the LEIS and XPS studies of metals (Cu,⁷ Fe,⁶ Pt,⁸ and Au) on TiO₂ (110), we can draw some conclusions

regarding their growth behavior at high metal coverages (>1 ML). Fe and Pt are reported to grow as "flat islands." Cu, like Au, at higher coverages, grows as "dropletlike islands," however, the Au/TiO₂ (110) system exhibits less wetting. Didier and Jupille⁴¹ calculated the adhesion energies, defined as the energy per unit area required to separate the interface, for metal on oxides. Their calculations show the reactive strength of the adhesion energy, for Fe, Au, and Cu on both SiO₂ and Al₂O₃ substrates, to be in the order Au < Cu < Fe. This is in the same order as the wetting ability. The lower the wetting, the less work is needed to separate the two surfaces. XPS results show that Fe is partially oxidized at the Fe/TiO₂ interface,⁶ while no indication of strong interfacial reactions has been found for Cu, Pt, and Au.

After annealing Fe (Ref. 27) and Pt/TiO₂ (Ref. 28) to 800 K in UHV, strong evidence for encapsulation of Fe and Pt islands by Ti suboxides has been observed. The Au/TiO₂ system shows better thermal stability and no encapsulation is found upon annealing to the same temperature in UHV. This suggests that, in order to have encapsulation, the metal should be reactive enough to cause the decomposition of TiO₂ to TiO_x ($x < 2$). Au is relatively inert and does not show any encapsulation upon annealing.

V. SUMMARY

For substrate temperatures of 160 and 300 K, Au initially grows as quasi-two-dimensional islands on TiO₂ (110) at fractional monolayer coverage. When the average Au coverage increases, Au forms three-dimensional islands. The transition from quasi-2D growth to 3D may also be accompanied by band bending in TiO₂ at low Au coverages. At 475 K, Au initially forms 3D islands. There is no indication of a strong interface reaction at any Au coverage or substrate temperature. The Au islands grow either larger or thicker as the surface temperature increases. The LEED studies indicate that Au grows along the fcc (111) orientation.

A search for adsorption of CO on small Au clusters shows that little or no CO adsorbs on very small Au clusters (average Au coverage < 1 ML). Our results give an upper limit on CO chemisorption on Au at 300 K of $\sim 5\%$ of a monolayer.

The annealing of Au/TiO₂ to temperatures as high as 775 K results in less substrate area being covered after annealing, due to island growth or thickening, but there is no evidence for encapsulation of Au by titanium suboxides, as reported for other metals.

*Present address: KLA-TENCOR, Milpitas, CA 95035.

[†]Author to whom correspondence should be addressed. FAX: (732) 445-4991. Electronic address: madey@physics.rutgers.edu

¹R. J. Lad, Surf. Rev. Lett. **1**, 109 (1995).

²A. M. Azad, S. A. Akbar, S. G. Mhaisalkar, L. D. Birkefeld, and K. S. Goto, J. Electrochem. Soc. **139**, 3690 (1992).

³U. Kirner *et al.*, Sens. Actuators B **1**, 103 (1990).

⁴J.-M. Pan, B. L. Maschhoff, U. Diebold, and T. E. Madey, Surf. Sci. **291**, 381 (1993).

⁵U. Diebold, J.-M. Pan, and T. E. Madey, Surf. Sci. **331/333**, 845 (1995).

⁶J.-M. Pan and T. E. Madey, J. Vac. Sci. Technol. A **11**, 1667 (1993).

⁷U. Diebold, J.-M. Pan, and T. E. Madey, Phys. Rev. B **47**, 3868 (1993).

⁸H.-P. Steinrück, F. Pesty, L. Zhang, and T. E. Madey, Phys. Rev. B **51**, 2427 (1995).

⁹J.-M. Pan, U. Diebold, L. Zhang, and T. E. Madey, Surf. Sci. **295**, 411 (1993).

¹⁰R. Persaud and T. E. Madey, *The Chemical Physics of Solid Surfaces and Heterogeneous Catalysis*, edited by D. A. King and D. P. Woodruff (Elsevier, Amsterdam, 1997), Vol. 8.

¹¹T. Kobayashi, M. Haruta, H. Sano, and M. Nakane, Sens. Actuators **13**, 339 (1988).

¹²S. D. Lin, M. Bollinger, and M. A. Vannice, Catal. Lett. **17**, 245 (1993).

¹³S. Lin and M. A. Vannice, Catal. Lett. **10**, 47 (1991).

¹⁴M. Haruta, N. Yamada, T. Kobayashi, and S. Iijima, J. Catal. **115**, 301 (1989).

¹⁵D. M. Cox, R. Brickman, K. Creegan, and A. Kaldor, Z. Phys. D **19**, 353 (1991).

¹⁶Y. M. Sun, D. N. Belton, and J. M. White, J. Phys. Chem. **90**, 5178 (1986).

¹⁷M. J. Kelley, D. R. Short, and D. G. Swartzfager, J. Mol. Catal. **20**, 235 (1983).

¹⁸B. L. Maschhoff, J.-M. Pan, and T. E. Madey, Surf. Sci. **259**, 190 (1991).

¹⁹J. M. Pan, B. L. Maschhoff, U. Diebold, and T. E. Madey, J. Vac. Sci. Technol. A **10**, 2470 (1992).

²⁰E. Taglauer, in *Ion Scattering Spectroscopies for Surface Analysis*, edited by A. Czanderna and D. Hercules (Plenum, New York, 1991).

²¹K. H. Ernst, A. Ludviksson, R. Zhang, J. Yoshihara, and C. T. Campbell, Phys. Rev. B **47**, 13 782 (1993).

²²E. Bauer and J. H. van der Merwe, Phys. Rev. B **33**, 3657 (1986).

²³D. P. Woodruff and T. A. Delchar, in *Modern Techniques of Surface Science*, edited by R. W. Cahn, E. A. Davis, and I. M. Ward (Cambridge University Press, Cambridge, 1986).

²⁴A. G. Sault, R. J. Madix, and C. T. Campbell, Surf. Sci. **169**, 347 (1986).

²⁵A. Krozer and M. Rodahl (unpublished).

²⁶R. Dalven, *Introduction to Applied Solid State Physics* (Plenum, New York, 1980).

²⁷J.-M. Pan and T. E. Madey, Catal. Lett. **20**, 269 (1993).

²⁸F. Pesty, H.-P. Steinrück, and T. E. Madey, Surf. Sci. **339**, 83 (1995).

²⁹G. L. Haller and D. E. Resasco, Adv. Catal. **36**, 173 (1989).

³⁰L. Zhang, F. Cosandey, R. Persaud, and T. E. Madey (unpublished).

³¹B. Yakshinskiy, M. Akbulut, and T. E. Madey, Surf. Sci. (to be published).

³²D. Abriou, D. Gagnot, J. Jupille, and F. Creuzet, Surf. Rev. Lett. (to be published).

³³K. D. Schierbaum, S. Fischer, M. C. Torquemada, J. L. deSegovia, E. Roman, and J. A. Martin-Gago, Surf. Sci. **345**, 261 (1996).

³⁴H. Luth, *Surfaces and Interfaces of Solids* (Springer-Verlag, Berlin, 1993).

³⁵H. Onishi, T. Aruga, C. Egawa, and Y. Iwasawa, Surf. Sci. **233**, 261 (1990).

³⁶C. T. Campbell, Surf. Sci. Rep. **27**, 1 (1997).

- ³⁷A. W. Grant and C. T. Campbell, *Phys. Rev. B* **55**, 1844 (1997).
- ³⁸J. J. Métois, J. C. Heyraud, and R. Kern, *Surf. Sci.* **78**, 191 (1978).
- ³⁹F. Cosandey, R. Persaud, L. Zhang, and T. E. Madey, in *Structure and Evolution of Surfaces*, edited by E. H. Chason, T. L. Einstein, and E. D. Williams, MRS Symposium Proceedings No. **440** (Materials Research Society, Pittsburgh, 1997).
- ⁴⁰M. Zinke-Allmang, L. C. Feldman, and M. H. Grabow, *Surf. Sci. Rep.* **16**, 377 (1992).
- ⁴¹F. Didier and J. Jupille, *Surf. Sci.* **314**, 378 (1994).